Biometals (2010) 23:231–245
DOI 10.1007/s10534-009-9281-9

Effects of deferasirox and deferiprone on cellular iron load in the human hepatoma cell line HepaRG

François Gaboriau · Anne-Marie Leray · Martine Ropert · Lucie Gouffier · Isabelle Cannie · Marie-Bérengère Troadec · Olivier Loréal · Pierre Brissot · Gérard Lescoat

Received: 7 August 2009 / Accepted: 28 November 2009 / Published online: 8 December 2009

Abstract Two oral chelators, CP20 (deferiprone) and ICL670 (deferasirox), have been synthesized for the purpose of treating iron overload diseases, especially thalassemias. Given their antiproliferative effects resulting from the essential role played by iron in cell processes, such compounds might also be useful as anticancer agents. In the present study, we tested the impact of these two iron chelators on iron metabolism, in the HepaRG cell line which allowed us to study proliferating and differentiated hepatocytes. ICL670 uptake was greater than the CP20 uptake. The iron depletion induced by ICL670 in differentiated cells increased soluble transferrin receptor expression, decreased intracellular ferritin expression, inhibited ^{55}Fe (III) uptake, and reduced the hepatocyte concentration of the labile iron pool. In contrast, CP20 induced an unexpected slight increase in intracellular ferritin, which was amplified by iron-treated chelator exposure. CP20 also promoted Fe(III) uptake in differentiated HepaRG cells, thus leading to an increase of both the labile pool and storage forms of iron evaluated by calcein fluorescence and Perls staining, respectively. In acellular conditions, compared to CP20, iron removing ability from the calcein-Fe(III) complex was 40 times higher for ICL670. On the whole, biological responses of HepaRG cells to ICL670 treatment were characteristic of expected iron depletion. In contrast, the effects of CP20 suggest the potential involvement of this compound in the iron uptake from the external medium into the hepatocytes from the HepaRG cell line, therefore acting like a siderophore in this cell model.

Keywords Iron chelation · Iron metabolism · Siderophore · Hepatocytes · HepaRG cell line · Cell proliferation

Abbreviations

DFO	Desferrioxamine
MEM	Minimum essential medium
LDH	Lactate dehydrogenase
SDH	Succinate dehydrogenase
MTT	3-(4,5-Dimethylthiazol-2yl)2,5-diphenyl tetrazolium bromide
DMSO	Dimethyl sulfoxide
PBS	Phosphate-buffered saline
HBSS	Hank's buffered saline solution

F. Gaboriau (✉) · A.-M. Leray · M. Ropert · L. Gouffier · I. Cannie · M.-B. Troadec · O. Loréal · P. Brissot · G. Lescoat
Inserm U991 (EA/MDC), Université de Rennes 1, Hôpital Pontchaillou, 35033 Rennes Cedex, France
e-mail: francois.gaboriau@univ-rennes1.fr

M. Ropert
Laboratoire de Biochimie Générale et Enzymologie, Hôpital Pontchaillou, 35000 Rennes, France

P. Brissot
Service des Maladies du Foie, Hôpital Pontchaillou, 35000 Rennes, France

Introduction

Iron plays a key role in the regulation of many cell functions due to its involvement in redox processes. This metal is therefore an essential element for all living species. Dysregulation of iron metabolism may lead to iron overload as observed in genetic hemochromatosis (Brissot et al. 2008) and in thalassemia (Rund and Rachmilewitz 2005). Iron overload can have a damaging effect on many organs, especially the liver, pancreas and heart. It can also favor the development of liver cancer. Numerous iron chelators have been synthesized in order to treat human iron overload. Desferrioxamine (DFO) has, for a long time, been the sole compound useful for the treatment of iron overload. However, the need for parenteral administration has been a major handicap. Furthermore, continuous exposure to DFO causes a dose and time-dependent cytotoxicity (Valle et al. 1995). Designing orally active agents has thus become a major therapeutic challenge. Deferiprone (CP20, Fig. 1), the first orally active iron chelator available for clinical use (Al-Refaie et al. 1992; Collins et al. 1994; Olivieri et al. 1992), was hampered by a rare but unpredictable risk of neutropenia. More recently, ICL670 (deferasirox) has been successfully tested in the treatment of secondary iron overload of hematological origin (Cappellini et al. 2006).

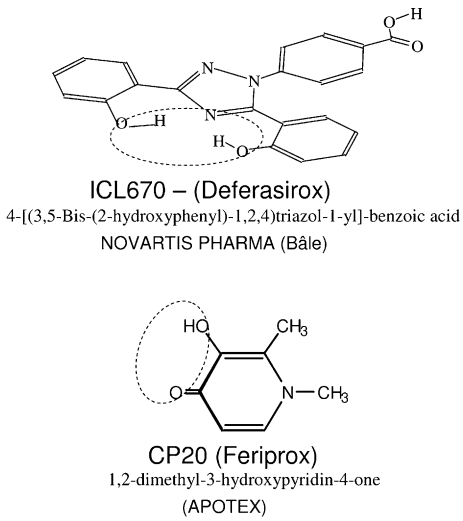

Fig. 1 Chemical structure of the iron chelators ICL670 or deferasirox (4-[(3,5-*bis*-(2-hydroxyphenyl)-1,2,4)triazol-1-yl]-benzoic acid) and CP20 or feriprox (1,2-dimethyl-3-hydroxypyridin-4-one)

The fact that tumor cells require high iron levels to ensure their proliferation (Richardson 1997) suggests these iron chelators might also be of clinical interest as potential antitumor agents. Iron chelators might help prevent the development of hepatocellular carcinoma and/or limit the proliferation of tumor cells (Brissot and Loreal 2002). Along this line, we previously reported the iron mobilization and the cytoprotective effect of CP20 in normal rat hepatocyte cultures (Chenoufi et al. 1995), and more recently an antiproliferative effect in the human hepatoblastoma cell line HepG2 (Chenoufi et al. 1998). In addition, in rat hepatoma cell line FAO and human hepatoma cell line HUH7 cultures, our results suggested that ICL670 has a higher antiproliferative effect due to its conjugated effects on both iron and polyamine metabolisms, two essential components involved in the control of cell proliferation (Lescoat et al. 2007). ICL670 inhibits polyamine biosynthesis by decreasing ornithine decarboxylase mRNA levels. In contrast, CP20 increases polyamine biosynthesis, especially putrescine levels, by stimulating spermidine-spermine *N*1-acetyl transferase activity that could activate the polyamine retro-conversion pathway.

The HepaRG cell line, developed in our laboratory, was isolated from a liver tumor of a patient suffering from a hepatocellular carcinoma (Gripon et al. 2002). This bipotent cell line differentiates progressively into both hepatocyte-like cells expressing highly differentiated functions and biliary-like cells. Our group used a transcriptomic approach to characterize this cell line and demonstrate its ability to store iron within hepatocytes, when differentiated (Troadec et al. 2006). Our aim was, using the HepaRG cell line, to evaluate the respective impact of both oral iron chelators, deferasirox and deferiprone, on hepatocyte iron metabolism, cell proliferation and differentiation.

Methods

Reagents

The cell-permeant form of Calcein, calcein-acetoxymethyl ester (CAL-AM) was obtained from molecular probes (Leiden, Holland). All other reagents, which were of the highest available grade, were

obtained from Sigma–Aldrich Chimie (Saint Quentin Fallavier, France).

Chelator solutions

Tridentate hydroxyphenyltriazole ICL670 (Deferasirox, Exjade from Novartis Pharma) (Rouan et al. 2001) and bidentate hydroxypyridinone CP20 (Deferiprone from Apotex) were compared. Stock solutions of each molecule (10 mM) were prepared in dimethyl sulfoxide (DMSO). The chelator concentration 100 μM corresponded to an addition in the culture medium of 1% DMSO which was preliminary verified to be inefficient on HepaRG cell viability. However, a low but significant cytotoxicity, giving rise to a decrease in SDH activity (−20%), was observed with 2% DMSO. This percentage was reached for chelator concentrations of 200 μM.

When chelator treatment was performed in presence of exogenous iron, the solution was iron saturated with ferric iron ($FeCl_3$) in stoichiometric conditions of chelation, one mole of iron for two or three moles of ICL670 or CP20, respectively. Unbound iron was not removed from the medium. NTBI is a form of iron which is found in the plasma of iron loaded patients during thalassaemia and genetic hemochromatosis. NTBI is classically used to induce iron overload in various cells because it corresponds to the plasma iron species which is mainly responsible for creating parenchymal (especially hepatocyte) iron deposition in human chronic iron overload.

Cell cultures

HepaRG cells were isolated from a liver tumor of a female patient suffering from hepatocarcinoma and hepatitis C infection (Gripon et al. 2002). HepaRG cells plated at 2×10^4 cells cm^{-2} in the presence of insulin and corticosteroids proliferated for 3–4 days with a doubling time of 24 h. During the proliferation phase, undifferentiated HepaRG cells appeared as a homogeneous epithelial phenotype cell population without regular structural organization. Progressive morphological changes, including the appearance of granular polygonal hepatocyte-like cells and flat clear epithelial cells, occurred after reaching confluency 2 weeks after plating.

Addition of 1.5% DMSO to the medium, 2 weeks after plating, potentiated the cell differentiation in two cell subtypes; (1) hepatocyte-like cells organized in well delineated trabeculae with many functional bile canaliculi-like structures similar to those observed in primary human hepatocyte culture, (2) a few clear flat epithelium-like cells filling the empty spaces around hepatocyte-like cells. Maximal cell differentiation, evidenced by these morphological changes and various functional markers, was reached after a 2-week DMSO exposure. The HepaRG cell model was chosen because offers the advantage of a cell line which is easily maintained in culture, and expresses practically all the liver-specific functions of cultured primary human hepatocytes: among them, apical and canalicular ABC transporters and basolateral solute carrier transporters, and production of albumin, haptoglobin as well as aldolase B gene expression which are specific markers of adult hepatocytes. HepaRG cells were cultured as previously described (Gripon et al. 2002). They were maintained in William's E medium supplemented with 10% fetal bovine serum, 100 U ml^{-1} penicillin, 100 μg ml^{-1} streptomycin, 5×10^{-5} M hydrocortisone hemisuccinate and 5 μg ml^{-1} insulin. Confluent cells at D15 were added with 1.5% DMSO to potentiate HepaRG differentiation.

Cells were seeded at 2×10^4 cells cm^{-2} in 96-well microplates for lactate dehydrogenase (LDH) and succinate dehydrogenase (SDH) measurements, in 24-well microplates for intracellular calcein measurements and in 6-well microplates for all other experiments.

Cell treatments

Three independent replicates were performed for each experiment and each experiment was repeated three times. Data reported are the mean results of three independent experiments.

Chelator exposures were performed at days 4 and 21 after cell seeding in 6-well microplates. After 72 h incubation at 37°C, 3 ml of cell supernatants were collected. Before biochemical analysis, including LDH, albumin and soluble transferrin, these supernatants were concentrated tenfold by ultrafiltration on Vivaspin™ spin columns with a membrane cut-off of 3,000 Da (Vivascience, France). The HepaRG cells were washed twice with sodium phosphate buffer 50 mM pH 7 and the cells were scraped and collected in 1 ml PBS and centrifuged 10 min at 1,500*g*. The

cell pellets were sonicated for 30 s at 4°C in 600 µl of an homogenization buffer, containing Tris–HCl 25 mM (pH 7.5), Dithiotreitol (1 mM), EDTA (0.1 mM) and Brij 35 (0.02%). These cell lysates were centrifuged at 10,000*g* for 10 min prior to biochemical analysis, including protein level, alkaline phosphatase activity and ferritin concentration measurements.

Comparison of chelator efficiency in aqueous phase

The cellular labile iron pool (LIP) is a pool of chelatable and redox-active iron, which plays a key role as a crossroad of cell iron metabolism. The ability of iron chelators to mobilize this temporary iron pool bound to low-molecular weight/low-iron affinity chelators (citrate, ascorbate, phosphate and adenosine triphosphate) is an essential factor influencing their biological efficiency.

In solution, calcein, a fluoresceinated analog of EDTA, binds Iron(II) and more slowly Iron(III) ($K_a = 1{,}024\ M^{-1}$). The fluorescence of this metallosensor dye is quenched during its interaction with iron and conversely is restored during removal of iron from the [calcein-iron] complex by various chelators. The rate and extent of fluorescence recovery depend on the chelator concentration, the kinetic and stoichiometry of iron binding and the relative binding affinity. Fluorescence ($\lambda_{Exc} = 485$ nm, $\lambda_{Em} = 520$ nm) of calcein (100 nM) in a HEPES buffer (20 mM HEPES, 150 mM NaCl, pH 7.3) was measured as a function of time, at room temperature, in a microplate fluorescence reader (Packard, Fusion^{TM}). Iron(III) (1 µM) slowly reacted with calcein and maximal quenching of its fluorescence was observed for time longer than 6 h. The kinetics of fluorescence recovery was monitored for 1 h, in presence of various chelator concentrations and the initial rate of the dequenching was deduced from the kinetics curves.

Cytochemical location of iron in HepaRG cell cultures

Fluorescence quenching of calcein

Calcein fluorescence quenching by iron was previously used for assessing the intracellular labile iron pool (LIP) and for measuring the iron chelator activity in living cells (Glickstein et al. 2006; Glickstein et al. 2005). Due to the cytoplasmic compartmentalization of this fluorescence dye, this method cannot be used to quantify the total LIP because the largest iron pool is lysosomal and remains inaccessible to free acid calcein (Tenopoulou et al. 2007). In the present study we used this fluorescent staining not to quantify the labile iron pool but to visualize, by microspectrofluorimetry, iron distribution between the two cell sub-types in differentiated HepaRG cell cultures and to compare the capacity of the two chelators to restore calcein fluorescence in hepatocytes and biliary-like cells, respectively.

HepaRG cells at D21 were loaded during 30 min incubation at 37°C (5% CO_2) with the cell-permeant dye calcein-acetoxymethyl ester (CAL-AM, 0.2 µM) in the cell culture medium. They were washed twice with PBS. Cell esterases released the fluorophore calcein and its fluorescence in cells was detected using the fluorescence-imaging microscope Axiovert 200 (Zeiss, Le Pecq, France). Image processing was performed with Axiovision 4.6 software.

Perls staining

Perls iron staining is the classical method for demonstrating iron deposits in tissues. After fixation with absolute alcohol, the differentiated HepaRG cells at D21 were treated with dilute hydrochloric acid to release ferric ions from binding proteins. These ions then reacted with potassium ferrocyanide to produce an insoluble blue compound (the Prussian blue reaction). In order to improve the contrast, nuclei were stained using nuclear red. Phase-contrast imaging was performed with an Axioskope Axiovision 4.6 microscope software (Zeiss, Le Pecq, France) and image processing with Simple PCI software.

Cytotoxic assays

Cytoxicity was evaluated by measuring extracellular lactate dehydrogenase activity (cytotoxicity detection kit—LDH, Roche, Penzberg, Germany) and mitochondrial succinate dehydrogenase activity (SDH) using the tetrazolium colorimetric assay (MTT, Sigma, St Louis, MO).

Extracellular LDH activity was measured as described by the manufacturer on a 20 µl aliquot of cell-free medium obtained by centrifugation (2,500 rpm min^{-1} during 5 min). LDH activities were detected by reading absorbance at 485 nm. An LDH standard curve (0–4,000 mU ml^{-1}) was used to quantify enzyme activity (L-lactate dehydrogenase, Sigma, St Louis, MO) and the values were corrected from the intracellular protein content measured according to the method of Bradford (1976). Data are the mean of three independent measurements. Extracellular LDH activity was reported as a percentage of the control value.

SDH activity was detected after 3 h incubation in 100 µl serum free medium containing 3-(4,5-dimethylthiazol-2-yl)-2,5-diphenyltetrazolium bromide (MTT, 0.5 mg l^{-1}). Formazan salts were solubilized with 200 µl DMSO and absorbance was read at 535 nm. Data are the mean of three independent measurements. SDH activity was reported as a percentage of the control value. Parameters of the dose–response curves were deduced from a 4-parameter curve fit according to Rodbard and McClean (1977)

$$y = \frac{(A_{c\,\min} - A_{c\,\max})}{1 + \left(\frac{C}{Cip}\right)^{\text{Pip}}} + A_{c\,\max}$$

in which y is the percentage of SDH activity with respect to the control, $A_{c\ \min}$ and $A_{c\ \max}$ are the y values observed for minimal and maximal chelator concentrations, respectively, C is the chelator concentration (C_{ip} at the inflection point) and P_{ip} is the slope at inflection point of the sigmoid curve. Due to their biphasic feature, the dose–response curves were fitted as the sum of two sigmoids (double 4-parameter fit). Percentages of HepaRG cells involved in each viability responses were deduced from the $A_{c\ \min}$, $A_{c\ \max}$ and IC50 values of each sigmoid, which were obtained from these fits.

Biochemical assays

The circulating sTfR concentration was previously shown to be proportional to cellular expression of the membrane-associated TfR and to increase with increased cellular iron needs (R'Zik and Beguin 2001). We used sTfR concentration measurements in cell supernatant as a marker of membrane TfR. Soluble Transferrin Receptor (sTfr) and albumin were quantified in concentrated supernatants by immunonephelemetry (BNII analyser, Dade Behring, Paris) using Dade Behring commercial kits, N latex sTfr reagent and N antiserum to human albumin, respectively.

The intracellular ferritin concentration was used as a marker of storage iron compartment. Intracellular ferritin concentration was measured with ADVIA Centaur Ferritin Assay Reagent and an ADVIA Centaur Analyzer (Bayer Diagnostics).

The intracellular alkaline phosphatase activity and the albumin secreted in cell supernatants were used to follow the loss of pluripotency of progenitor and the HepaRG cell differentiation, respectively, in functionally efficient hepatocytes. Intracellular alkaline phosphatase activity was measured with an Olympus AU 2700 auto analyzer (Olympus, Rungis) by standard enzymatic method using *p*-nitrophenyl phosphate (PNPP) as the substrate (Olympus reagent).

Chelator uptake measurement

Chelator uptake was investigated in HepaRG cell cultures seeded in 25 cm^2 culture flasks (20,000 cells cm^{-2}). Cell treatments were performed in triplicate, in proliferating cells (D4) or after differentiation (D21), with or without 60 µM CP20 or 40 µM ICL670. After 72 h of treatment, supernatants were removed and cells were then washed three times with 3 ml of ice-cold PBS solution. They were collected by scraping after adding 1 ml of water and sonicated for 30 s at 0°. Protein content in these cell extracts was measured by the Bradford method (Bradford 1976). Ultrafiltration of 200 µl of the cell lysates was performed by centrifugation for 20 min at 15,000*g* in NANOSEP™ 3 K centrifugal device (Pall Filtron Co).

Both chelators, CP20 and ICL670, were quantified by mass spectrometry analysis (positive mode) by monitoring the selective $[CP20 + H]^+$ ion at $m/z = 140.1$ and the $[ICL670 + H]^+$ ion at $m/z = 374.1$, which were generated with an Atmospheric Pressure Chemical Ionization (APCI) source (Gaboriau et al. 2004). No ion was observed at these masses in the mass spectra of the cell lysates obtained from control untreated HepaRG cells. Cell lysate samples (50 µl) were directly injected in the auto-sampler of the HP

1100 mass spectrometry analyzer, which was supplied with Chem-Station 1100 software (Agilent Technologies). The injection was performed into a stream of acetonitrile/water (3:1, v/v) at a flow rate of 0.5 ml min^{-1}. Selected ion monitoring (SIM) mode data masses were obtained using the full injection analysis (FIA) mode, without chromatographic separation. The following parameters were used: capillary voltage, +3,000 V; corona current, 5 μA; drying gas flow rate, 6 l min^{-1}; drying gas temperature, 300°; vaporizer temperature, 400°; nebulizer pressure, 30 psig; fragmentor voltage, 80 V. Areas under the ionic signals at $m/z = 140.1$ (CP20) and at $m/z = 374.1$ (ICL670) were integrated and chelator concentrations were then deduced by using the calibration curves obtained from cell lysate enrichments with various concentrations of the two chelators followed by their sonication and ultrafiltration. Each chelator measurement, which was performed as triplicate, was corrected from the protein content in the cell extracts.

^{55}Fe(III) uptake measurement

Iron(III) uptake was investigated in HepaRG cell cultures seeded in 24-well microplates (20,000 cells cm^{-2}). Cell treatments with 10 μM ^{55}Fe(III) (chloride or citrate salts) were performed in triplicate, in proliferating cells (D4) or after differentiation (D21), with or without 60 μM CP20 or 40 μM ICL670. After 72 h of treatment, the supernatants were collected for LDH measurements and the cells were then washed twice with 0.5 ml of ice-cold PBS solution and lyzed by sonication (30 s at 0°C) in 0.5 ml of PBS. Radioactivity in an aliquot of 0.3 ml of cell extracts was counted in 3 ml of scintillation liquid using a Packard Tricarb (2100TR) radioactive scintillation analyzer. The iron(III) concentration was deduced from a calibration curve and was corrected for cell extract protein content.

Statistical analysis

Results from at least four replicates were expressed as means ± SD. Statistical analysis was performed using the Mann–Whitney test. $P < 0.05$ was considered significant.

Results

Comparison of chelator efficiency

In acellular condition, the efficiency of both chelators CP20 and ICL670 to remove the iron from the [calcein-iron(III)] complexes was monitored by calcein fluorescence dequenching. The initial rate of this rise in calcein fluorescence was measured in the aqueous phase for 30 min after the addition of the two chelators and reported as a function of the chelator concentration in Fig. 2. The chelator concentration inducing 50% of the maximal rise in calcein fluorescence intensity was 40-fold lower for ICL670 (0.43 μM) than for CP20 (17 μM), suggesting the higher chelating efficiency of ICL670 compared with CP20.

Cytotoxic and antiproliferative effects of chelators

Dose–response curves, obtained from ICL670 and CP20, could not be described as simple sigmoids and suggested two distinct effects of these two chelators

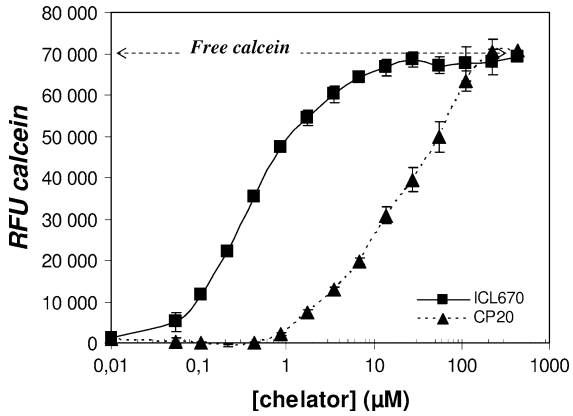

Fig. 2 Comparison of iron chelating efficiency by using calcein fluorescence measurements in a cell-free system. Fluorescence of 100 nM calcein ($\lambda_{Exc} = 485$ nm, $\lambda_{Em} = 520$ nm) in Hepes buffer (20 mM Hepes, 150 mM NaCl, pH 7.3) was detected in a microplate fluorescence reader (free calcein). Iron(III) (1 μM) quenched the calcein fluorescence and addition of both chelators ICL670 (*filled triangle*) and CP20 (*filled square*) led to a fluorescence recovery depending on the chelator concentration, the kinetics and stoichiometry of their iron binding and their relative binding affinity

on cell viability at low concentrations (between 1 and 20 μM) and for concentrations higher than 20 μM, respectively. The effect observed for low chelator concentrations, reversed in presence of iron-treated chelator, was not associated to cell membrane damage (no LDH increase). This effect could be the result of the antiproliferative effect induced by iron-depletion. To determine the antiproliferative effect of ICL670 and CP20 in proliferating HepaRG cells treated at day 4 (Fig. 3a), the dose–response curves for the chelators were fitted as a double four-parameter fit in order to calculate the percentage of cells involved in each cell viability decrease, as well as the corresponding IC50 s of the chelators. The antiproliferative effect of ICL670 (IC50 = 6.5 μM) and CP20 (IC50 = 15 μM) involves, respectively, 65 and 20% of the HepaRG cells of the cultures. The number of cell nuclei determined by Hoechst stain microfluorimetry showed that the decrease in succinate-dehydrogenase activity in this range of concentrations was due to a decrease in the number of viable cell (data not shown). As deduced from the absence of LDH leakage in supernatants (Fig. 3b), the chelator treatments in this range of concentration (<20 μM) were not cytotoxic. The addition of 20 μM iron(III) in the culture medium increased the mitochondrial succinate dehydrogenase concentration (20%) for chelator concentrations lower than 20 μM. Absence of any increase in the Hoechst stain cell nuclei count showed that cell proliferation was not the source of this increase (data not shown). The decrease in cell viability observed at low chelator concentration (<60 μM) was totally reversed by addition of 20 μM iron(III)-treated chelator. The decrease in cell viability for chelator concentrations higher than 100 μM (Fig. 3a) was associated with LDH leakage in cell supernatants (Fig. 3b) and was probably due to the cytotoxic effects of both chelator and DMSO.

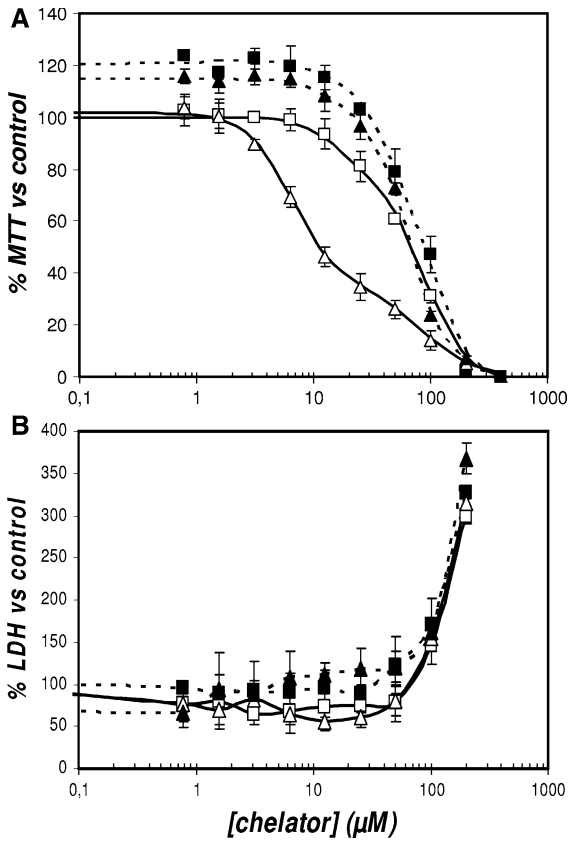

Fig. 3 Effect of chelators on cell viability (**a** MTT assay) and cytotoxicity (**b** LDH release in cell supernatant) in proliferating HepaRG cell cultures. HepaRG cells at D4 were maintained in culture for 72 h with various concentrations of ICL670 (*open triangle*) or CP20 (*open square*) in presence (*filled symbol*) or absence (*open symbol*) of 20 μM Fe(III)

Hexacoordination of one atom of Fe(III) with the chelators required three and two molecules of bidentate CP20 and tridentate ICL670, respectively. Therefore, for this comparative study of the biological efficiency of CP20 and ICL670, the sub-toxic chelator concentrations were chosen in the ratio of their stoichiometric interaction with 20 μM iron(III) ([ICL670] = 40 μM, [CP20] = 60 μM).

The basal values of protein concentrations in untreated control HepaRG cells at the various steps of cell growth (Table 1) reached a maximal value when cells were confluent at day 15 (data not shown) and remained constant after cell differentiation at day 21. Exogenous iron contained in the cell culture medium appeared to be a limiting factor when cells were proliferating, as deduced from the 50% increase in the protein level at day 4, in presence of 20 μM iron(III). Treatment with both chelators at comparable iron binding equivalent concentrations induced a decrease in protein content (43 and 56% of control for ICL670 and CP20, respectively) in proliferating cells (D4), and in differentiated cells at D21 (74 and 44% of control for ICL670 and CP20, respectively). These inhibiting effects of chelators at D4 and D21 were reversed in presence of 20 μM iron(III)-treated chelator.

Table 1 Effect of 40 μM ICL and 60 μM CP20 after 72 h of incubation, in the presence or absence of 20 μM Fe(III), on protein and alkaline phosphatase cell contents, and on albumin in supernatants of HepaRG cell cultures at D4 and D21

	Percentage vs. control (values)					
	Control		ICL670A		CP20	
	−Fe(III)	+Fe(III)	−Fe(III)	+Fe(III)	−Fe(III)	+Fe(III)
Protein (g l^{-1})						
D4	100 ± 15 (0.100)	151 ± 9 (0.151)*	43 ± 3 (0.043)*	96 ± 9 (0.096)	56 ± 14 (0.056)*	89 ± 13 (0.089)
D21	100 ± 2 (0.301)	111 ± 7 (0.334)*	74 ± 16 (0.222)*	98 ± 11 (0.295)	44 ± 8 (0.132)*	109 ± 6 (0.328)
Albumin (mg g^{-1})						
D4	100 ± 18 (316)	88 ± 8 (278)	115 ± 4 (363)	96 ± 28 (303)	161 ± 13 (509)*	129 ± 11 (408)
D21	100 ± 2 (1,214)	98 ± 3 (1,190)	57 ± 23 (692)*	102 ± 22 (1,238)	60 ± 6 (728)*	97 ± 11 (1,178)
Alkaline phosphatase (U g^{-1})						
D4	100 ± 4 (292)	98 ± 18 (286)	67 ± 22 (196)*	93 ± 3 (272)	115 ± 2 (336)*	84 ± 10 (245)
D21	100 ± 6 (113)	129 ± 13 (146)	187 ± 5 (211)*	107 ± 9 (121)	221 ± 3 (250)*	121 ± 1 (137)

Results were expressed as percentages of control values while actual values were given in parentheses

* Statistically different from control, according to the Mann–Whitney test ($P < 0.05$)

Effects of chelators on HepaRG differentiation

The bipotent HepaRG cell line progressively trans-differentiated in both hepatocyte-like cells expressing highly differentiated functions, including albumin expression, and biliary epithelial-like cells (Cerec et al. 2007; Gripon et al. 2002). As other pluripotent embryonic stem cells, HepaRG bipotent progenitors express markers of in vivo hepatic progenitors including alkaline phosphatase activity (Ruhnke et al. 2003) and cell differentiation processes associated with a loss of their expression (Cerec et al. 2007).

Differentiation of untreated control HepaRG cells in functionally efficient hepatocytes was associated with an increase in albumin secretion in cell supernatants (Table 1). Treatment of the proliferating cells at D4 by CP20 induced an increase in albumin secretion while both chelators induced an around 40% decrease in albumin in differentiated HepaRG cell culture at D21.

In the absence of treatment, the high alkaline phosphatase activity in proliferating bipotent cells decreased until HepaRG cells differentiated (Table 1). The more pronounced effect of chelators on alkaline phosphatase activity was observed in fully differentiated cells at D21 where this activity increased compared with controls (187 and 221% vs. control for ICL670 and CP20, respectively). Iron loading induced by 20 μM Iron(III) treatment weakly increased alkaline phosphatase activity and reversed the effect of chelators at D21.

Effects of chelators on iron metabolism

^{55}Fe(III) uptake measurement

^{55}Fe(III) uptake in the absence of chelator was slightly higher in differentiated HepaRG cells (D21, 12.4 μmol g^{-1}) than in proliferating cells (D4, 10.9 μmol g^{-1}) (Fig. 4). In proliferating cells, this uptake was inhibited in presence of 40 μM ICL670 (−80% with respect to control) and with 60 μM CP20 (−30%). In differentiated cells, ICL670 also inhibited ^{55}Fe(III) uptake (−80% compared with control), while it was enhanced in cells treated by 60 μM CP20 (+50% in HepaRG cell at D21).

Impact of iron chelators on soluble iron pool and iron storage forms

The two cell subtypes, differentiated hepatocytes and the biliary-like cells, were clearly discriminated by phase contrast microscopy analysis of differentiated HepaRG control cells at D21 (Fig. 5a). The analysis of calcein fluorescence of the same microscopic field (Fig. 5b), showed a lower fluorescence in the hepatocyte islets. Hepatocytes excluded the fluorescent

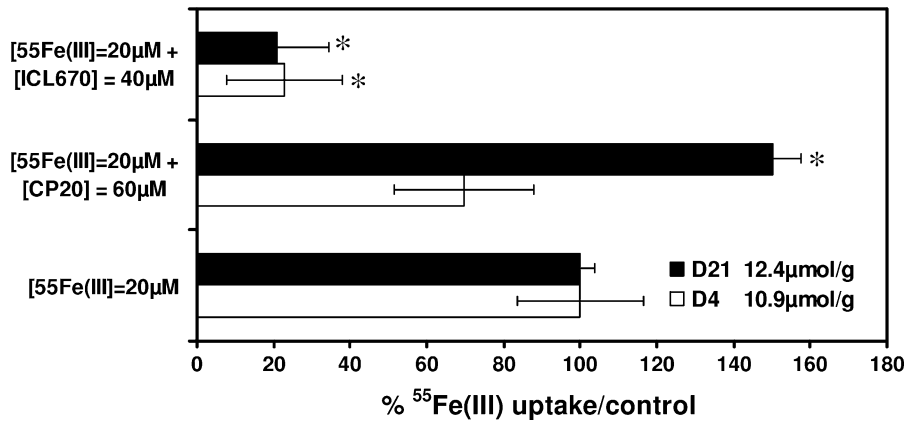

Fig. 4 Effect of 40 µM ICL and 60 µM CP20 on ^{55}Fe(III) uptake in HepaRG cells at D4 and D21. Results were expressed as percentages of control values reported in the insert of the figure. "*" Statistically different from control, according to the Mann–Whitney test ($P < 0.05$)

dye ethidium homodimer-1 and thus were perfectly viable (data not shown). Consequently, we concluded that the lower calcein fluorescence observed in hepatocytes was not due to toxic effects associated with a lack of intracellular esterase but resulted from the quenching of the calcein fluorescence due to a higher level of labile iron pool in these cells. This was confirmed by phase contrast microscopy analysis (Fig. 5c) and the corresponding fluorescence imaging of differentiated HepaRG cells (D21) loaded with calcein (Fig. 5d) and treated for 72 h with 40 µM ICL670. The uptake of ICL670 partially restored the calcein fluorescence in the hepatocyte islets and weakly increased the fluorescence in the biliary-like cells, particularly in perinuclear spots. The treatment of differentiated HepaRG cell cultures by 60 µM CP20 did not restore the calcein fluorescence in hepatocytes but weakly increased the fluorescence in biliary-like cells associated with a more pronounced hot-spot perinuclear labeling (Fig. 5e, f) shown with the higher magnification (×3) of one biliary-like cell inserted in Fig. 5f. A higher number of lysis areas (surrounded by dotted lines) associated with an hepatocyte toxicity islet was also observed with CP20.

Perls staining histochemical analysis of Fe(III) uptake

Iron loading of differentiated HepaRG cells (D21), induced by a 72 h incubation with 20 µM Fe(III) in the absence of chelator, enhanced the iron storage pathway and led to Prussian blue staining in the cytoplasm (Fig. 6a). It is generally considered that diffuse and granular iron staining correspond, respectively, to the iron storage in ferritin and hemosiderin. Iron loading of differentiated HepaRG cells (72 h incubation with 20 µM Fe(III)) in the presence of 60 µM CP20), mainly augmented diffuse staining (Fig. 6b). No such increase was observed in proliferating cells at D4 (data not shown). Iron loading with 40 µM ICL670 significantly reduced both granular and diffuse Prussian blue staining (Fig. 6c).

Soluble transferrin receptor

The sTfR concentrations (Fig. 7) were higher in proliferating HepaRG cells (D4) than in differentiated cells (D21). The iron depletion induced by both chelators led to a sharp rise in the sTfR concentrations in proliferating cells at D4 (3.7- and a 3.6-fold increase for ICL670 and CP20, respectively) and in differentiated cells at D21 (2.2- and a 3.4-fold increase for ICL670 and CP20, respectively). The addition of 20 µM exogenous Fe(III) reversed this effect totally at D4 and partially in differentiated cells.

Ferritin

Unlike the soluble transferrin receptor, the intracellular ferritin concentration was lower in proliferating HepaRG cells (D4) than in differentiated cells (D21) (Fig. 8a). Iron depletion induced by 72 h treatment with 40 µM ICL670 led to a decrease in iron storage capacity expressed by a decrease in ferritin level at all stages of the cell culture (−62 and −63% at D4 and D21, respectively). In contrast, treatment with CP20

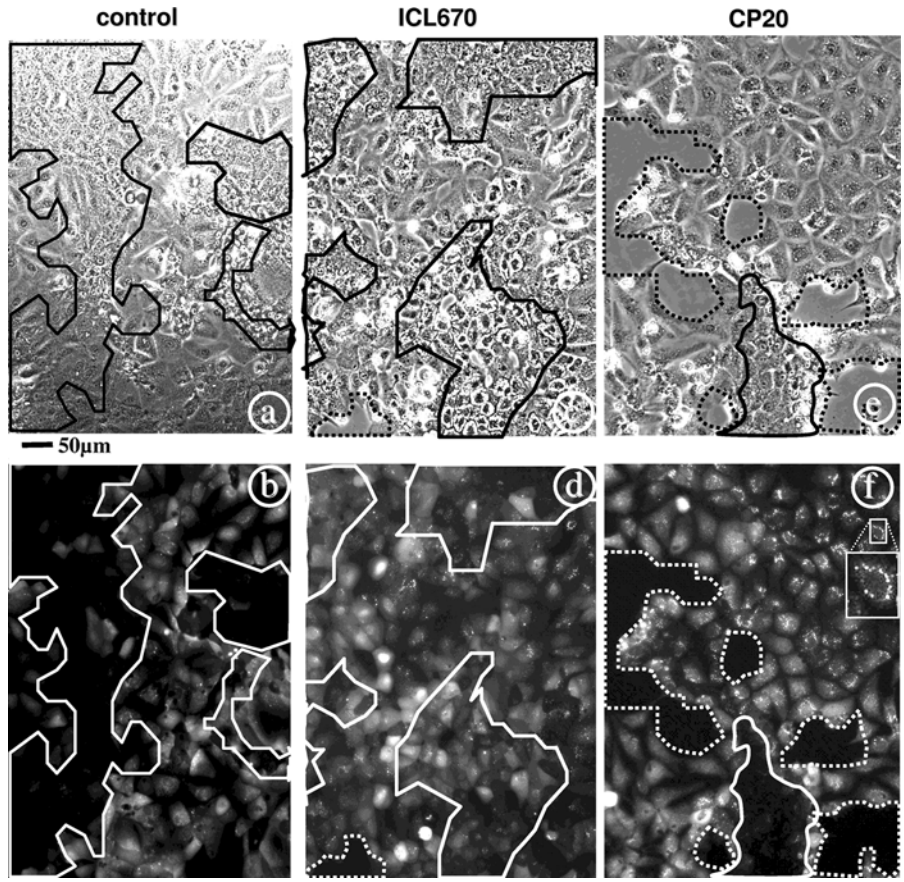

Fig. 5 Histochemical analysis, using the iron sensor calcein, of the effect of 72 h treatment with 40 µM ICL670 (**c**, **d**) or 60 µM CP20 (**e**, **f**) in differentiated HepaRG cells at D21. The two cell subtypes; differentiated hepatocytes-like (surrounded by *plain line*) and the biliary-like cells were clearly discriminated by phase contrast microscopy analysis. *Bar*: 50 µm. A higher magnification (×3) of one biliary-like cell was inserted in picture **f**

led to an increase in ferritin level (+40 and +64% at D4 and D21, respectively).

As shown in Fig. 8B, iron loading of HepaRG cells, induced by 72 h incubation with 20 µM Fe(III) in the absence of chelator, led to an increase in the intracellular ferritin level (15- and 20-fold increase at D4 and D21, respectively). The addition of 20 µM iron(III)-treated chelator, reversed the inhibiting effect of ICL670 on ferritin level while it amplified the activating effect of CP20 (4- and 23-fold increase at D4 and D21, respectively). At D4, the lower increase in ferritin level induced by iron-treated chelator in HepaRG proliferating cells, treated or not with CP20, confirmed that iron appeared to be a limiting factor during the proliferation stage. ^{55}Fe(III) uptake (Fig. 4) was linearly correlated with the ferritin level ($r = 0.98$, data not shown).

Measurement of chelator uptake by mass spectrometry

HepaRG cells at D4 and D21 were incubated for 72 h in the presence of 40 µM ICL670 or 60 µM CP20. ICL670 uptake was shown to be about twofold higher than that of CP20 in proliferating and differentiated HepaRG cells. At the end of the incubation, CP20 and ICL670 intracellular content (Fig. 9) were, respectively: 1.81 ± 0.37 and 3.47 ± 0.79 µmol mg^{-1} protein in proliferating cells, and 1.15 ± 0.23 and 3.93 ± 1.36 µmol mg^{-1} protein in differentiated HepaRG cells. The chelator uptake was

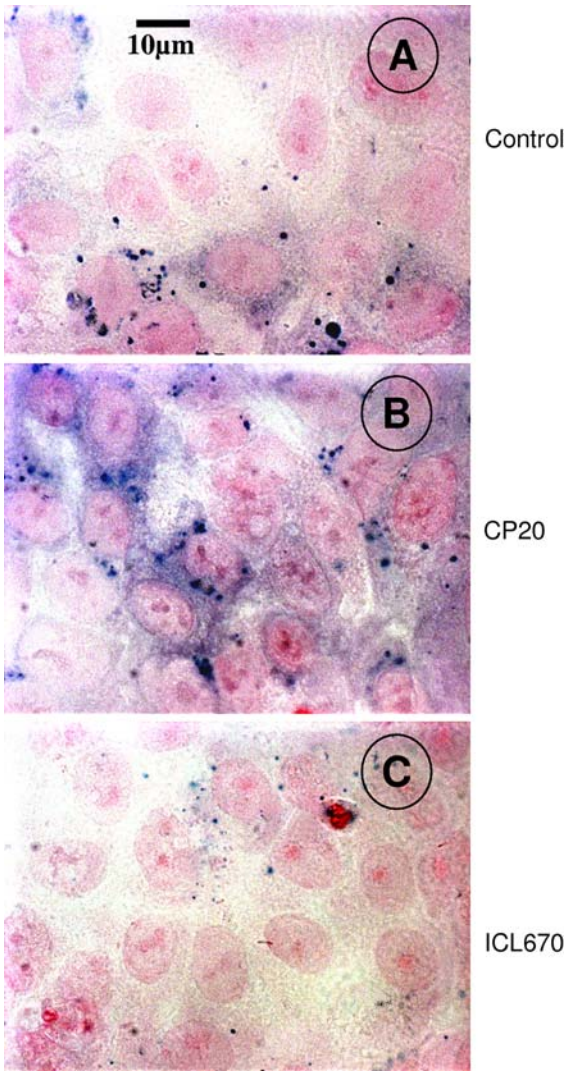

Fig. 6 Histochemical analysis, using Perls staining, of the effect of a 72 h treatment with 60 µM CP20 (**b**) or 40 µM ICL670 (**c**) in differentiated HepaRG cells at D21. A counter staining with nuclear red led to the red stain of nuclei and improved the contrast. Phase contrast microscopy analysis. *Bar*: 10 µM

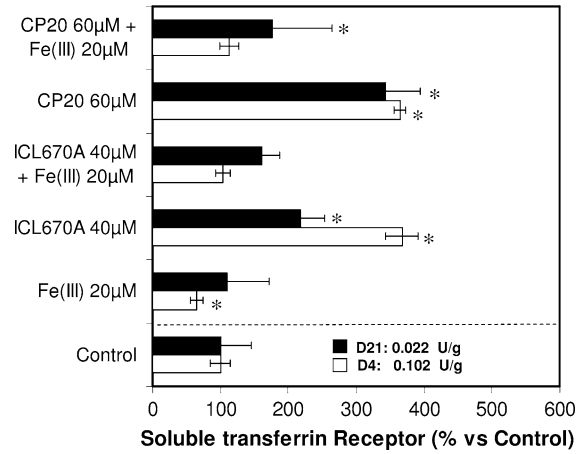

Fig. 7 Effect of 40 µM ICL and 60 µM CP20 after 72 h of incubation, in the presence or absence of 20 µM Fe(III), on soluble transferrin receptor in supernatants of HepaRG cell cultures at D4 and D21. Results were expressed as percentages of control values reported in the insert of the figure. "*" Statistically different from control, according to the Mann–Whitney test ($P < 0.05$)

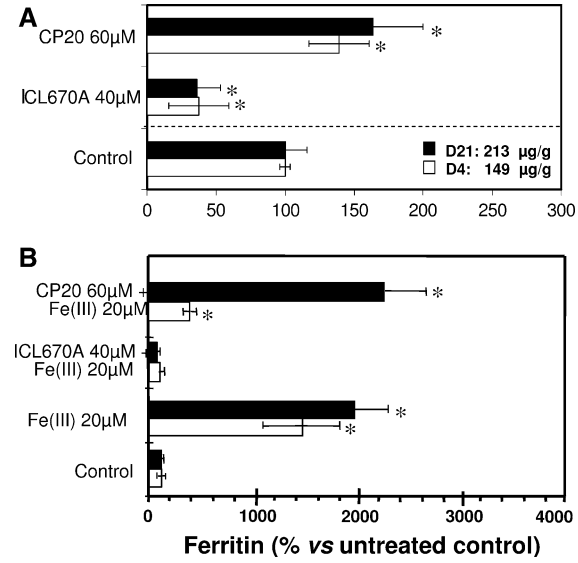

Fig. 8 Effect of 40 µM ICL and 60 µM CP20 after 72 h of incubation, in the presence (**b**) or absence (**a**) of 20 µM Fe(III), on intracellular ferritin content in HepaRG cells at D4 and D21. Results were expressed as percentages of control values reported in the insert of the figure. "*" Statistically different from control, according to the Mann–Whitney test ($P < 0.05$)

not modified by addition of iron-saturated chelator(III) (data not shown).

Discussion

Hepatocytes are a major target in iron overload diseases. Hepatic iron overload (Brissot et al. 1985; De Silva et al. 1996; Wright et al. 1986) is associated with fibrosis, cirrhosis, hepatocellular carcinoma (Deugnier et al. 1993; Turlin and Deugnier 2002).

Iron chelators are useful tools to achieve iron depletion in patients with iron overload, especially

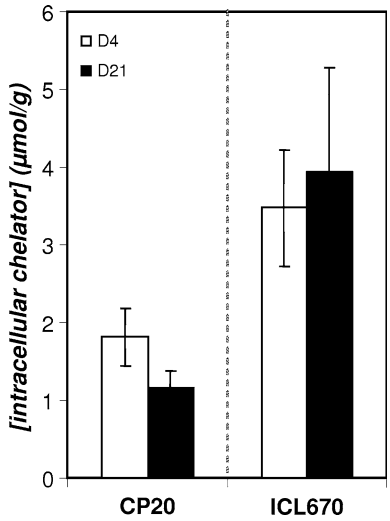

Fig. 9 Chelator uptake in HepaRG cells at D4 and D21. Intracellular chelator contents were measured by mass spectrometry after a 72 h incubation of the HepaRG cells with 40 µM ICL670 or 60 µM CP20

when linked to thalassemia. In addition, iron chelators have been reported to exert antiproliferative effects and have therefore been proposed as anticancer drugs (Richardson and Milnes 1997).

The HepaRG cell line (Gripon et al. 2002) is a bipotent cell line which differentiates progressively into both hepatocyte-like cells expressing highly differentiated functions and biliary-like cells. Transcriptomic analysis has been applied to characterize this cell line which, when differentiated, exhibits an ability to store iron within hepatocytes (Troadec et al. 2006). This model gave us the opportunity to test the influence of new oral iron chelators, deferiprone and deferasirox, on iron metabolism and proliferation in hepatocytes. Sub-toxic chelator concentrations tested in this study were chosen in the ratio of their stoichiometric interaction with 20 µM iron (60 µM CP20 and 40 µM ICL670). Such concentrations were close to those achieved in the plasma of chelated thalassemic patients. For CP20 (Deferiprone), with standard dosage (25 mg kg^{-1} three times per day), plasma chelator level was previously shown to peak within 1 h of intake to 100–200 µM, with an half-time of 2.5 h (Kontoghiorghes et al. 1990; Kushner et al. 2001), while with a single dose of 20 mg^{-1} Kg^{-1} day^{-1} of ICL670 (deferasirox), plasma level was reported to peak at 100 µM with an half-time of 12 h (Cappellini et al. 2006).

Microscopic analysis showed the more pronounced cytotoxic effect of both chelators against hepatocytes-like colonies in differentiated HepaRG cell cultures leading to lysis areas surrounded by biliary-like epitheloid cells (Fig. 6). This selective toxicity of both chelators against hepatocytes-like cells could explain the decrease in albumin secretion induced by chelator treatment in differentiated HepaRG cells (Table 1).

Iron metabolism during progression of the HepaRG cell line

We used proliferating and differentiated HepaRG cells at D4 and D21. Progression of cells toward a differentiated status was assessed by the decrease of alkaline phosphatase activity and the increase of the albumin secretion in cell supernatants. The latter result confirmed the previously reported increase in albumin RNA expression associated with hepatocytes-like cells differentiation (Gripon et al. 2002).

It is noteworthy that the low iron content in cell culture medium appeared to be a limiting factor for HepaRG cell metabolism. Indeed, iron loading with 20 µM Fe(III) increased cell protein content and the mitochondrial succinate dehydrogenase activity (MTT assay) 4 days after cell seeding, while the cytotoxic and cytostatic effects of iron depletion induced by CP20 and ICL670 was reversed by iron-treated chelator.

Hepatocytes are a major iron storage site for ferritin and hemosiderin (Theil 1987). Furthermore, the iron overload observed in human liver during genetic hemochromatosis is well known to primarily occur within hepatocytes while stainable iron in biliary-like cells is observed after a longer period of iron overload (Deugnier et al. 1992). Accordingly, after iron exposure, we detected higher iron concentrations in hepatocyte islets using both calcein fluorescence and Perls staining. Iron deposits were only found within hepatocytes-like cell cytoplasm. Iron excess was neither observed in proliferating cells at D4 nor in biliary-like epitheloid cells when the HepaRG cell culture differentiated (D21). These results confirm a previous transcriptomic study of this cell model showing that the HepaRG iron loading capacity is chronologically associated with the decrease in cell motility, which is a characteristic of

proliferating cells, and to the appearance of differentiated hepatocyte-like cells (Troadec et al. 2006).

Effect of iron chelators on iron metabolism

The pFe^{3+} of the various iron chelators was considered in order to compare the strength of the iron-chelator complexes. pFe^{3+} corresponds to the negative logarithm of the free iron concentration at pH 7.4 and in the presence of Fe(III) and chelator concentrations of 1 and 10 μM, respectively. Our comparison of the Fe(III)-chelating efficiency of both chelators, by using calcein fluorescence recovery in solution, indicated the 40-fold higher efficiency of ICL670 over CP20 for removing iron from [calcein-Fe(III)] complexes, which was in agreement with the previously reported pFe^{3+} values of chelators (25.4 and 20 for ICL670 and CP20, respectively) (Buss et al. 2003).

In HepaRG cell cultures, the fluorescence of the calcein dye was quenched in the hepatocyte-like cells islets, which exhibited higher levels of iron. The calcein fluorescence was restored in these cells by incubation in presence of ICL670 but remained quenched in presence of CP20. CP20 only restored the calcein fluorescence in biliary-like cells associated with hot-spot perinuclear labeling. In a recent study using the H9C2 cardiomyocyte cell line, Sohn et al. (2008) showed that calcein green dye (CALG) accumulated in endosomes and was co localized with classical fluid phase endocytosis markers. As observed in our study, the resulting calcein fluorescence, located in perinuclear spots, increased after incubation for 1 h in the presence of 50 μM CP20.

The absence of calcein fluorescence dequenching in the hepatocyte-like cells islets with CP20 could be due to its lower iron binding capacity as discussed above (Fig. 2) and/or to its twofold to threefold lower uptake in these cells compared to ICL670 (Fig. 9). The cellular uptake of both chelators was not modified by exogenous iron(III). In a previous work on the rat hepatocyte FAO cell line and using mass spectrometry measurements, ICL670 cellular uptake was shown to be six times higher than CP20 (Lescoat et al. 2007).

Ferritin and TfR synthesis are regulated at the post-transcriptional level by the intracellular Fe concentration, via the iron responsive elements (IRE) located in the 5′ or 3′ untranslated region (UTR) of ferritin and TfR mRNAs, respectively, and the iron regulatory proteins (IRP1 and IRP2) (Muckenthaler et al. 2008). In agreement with this regulation, we showed in the present work that iron overload increases ferritin levels (Fig. 8) and decreases soluble transferrin receptors (Fig. 7) in proliferating cells (D4) while it remains unchanged in differentiated cells (D21). This unexpected data could probably find an interpretation in the very low sTrf level (0.022 U g^{-1} protein) observed in the differentiated cells and reflects the detection limit of this parameter in this condition. Conversely, the iron depletion induced by the treatment with 40 μM ICL670 led to a decrease in ferritin level and to a concomitant increase in sTfR in cell supernatant in proliferating and differentiated HepaRG cells. As expected for an iron chelator, ICL670 also reduced the iron uptake which was confirmed by $^{55}Fe(III)$ uptake analysis (Fig. 4) as well as the fluorescence calcein histochemical analysis (Fig. 5) and Perls staining (Fig. 6). CP20, in the HepaRG cell model, was a poorly efficient iron chelator and could play the role of a siderophore in the presence of iron. Indeed, this compound induced a weak increase in ferritin level which was amplified in the presence of 20 μM iron(III). Further probes of the ability of CP20 to induce iron accumulation in cells were deduced from the Perls stain cytochemical analysis, reflecting iron storage forms, and calcein fluorescence, reflecting labile forms of iron. Finally, this compound was also shown to induce a twofold increase in $^{55}Fe(III)$ uptake in differentiated HepaRG cells.

Huang and collaborators (Huang et al. 2006), using the Caco-2 cell model cultured on permeable membrane, demonstrated that DFO, CP20 and ICL670 were passively transported across the enterocyte cell monolayer with a membrane permeability modulated by the lipophilicity and the charge of the chelators (CP20 > ICL670). The iron chelates $[Fe(ICL670)_2]$ and [Fe(DFO)] were not transported across Caco-2 monolayers, while the $[Fe(CP20)_3]$ chelate was able to cross the monolayer in both directions. Furthermore, CP20 was reported to remove iron efficiently from transferrin (Kontoghiorghes and Evans 1985) and from isolated ferritin (Kontoghiorghes 1986). These properties of CP20 and $[Fe(CP20)_3]$ chelates point out its peculiar cellular uptake probably related

to its low molecular weight associated with its relative lipophilicity.

Thus, our observations suggest that CP20 could act as a siderophore in the HepaRG cell model. Bacteria and fungi synthesize and secrete chelators as a means of acquiring iron from their environment (Albrecht-Gary and Crumbliss 1998). The best-known example of these natural siderophores is the chelator desferrioxamine. Such a mechanism could explain the increase in intracellular ferritin level, induced by CP20 alone and to a greater extent in the presence of iron (Fig. 8). Accordingly to this hypothesis, recent results from Sohn et al. (2008) showed the ability of CP20 to shuttle iron across cell membranes and to redistribute it between cellular organelles. By using fluorescence dye iron sensors, specifically located in various organelles, these authors demonstrated the involvement of CP20 in the intra- and inter-cellular transport of iron across membranes. The role of CP20 as a shuttle acting independently of transferrin was confirmed by its transfer capacity of iron from iron-loaded macrophages to pre-erythroid cells. The potential role of CP20 as a siderophore appears in contradiction with its reported applications for reducing myocardial iron burden and for normalizing cardiac function of thalassemia patients (Mamtani and Kulkarni 2008).

In conclusion, our study of the impact of the oral iron chelators, deferiprone (CP20) and deferasirox (ICL670), on iron metabolism in the HepaRG cell culture model demonstrates a higher chelating efficiency of deferasirox and an unexpected siderophore-like action of deferiprone. Due to the apparent contradiction with its reported clinical efficiency, the potential siderophore role of CP20, associated with iron overloading in HepaRG cells requires further investigations in other cell types. These in vitro data should be kept in mind when applying these compounds for the treatment of human Iron overload.

Acknowledgments This work was supported by the 6th PCRDT European contract EuroIron-1 (No 037296) "Genetic control of the pathogenesis of diseases based on iron accumulation", the French National Ligue contre le Cancer (35 and 44 Committees), the ACI CAPFER "nouveaux outils chimiques et analytiques pour la détection et le dosage du fer; application à l'étude de son métabolisme" No 032135 and the "Programme de Recherche d'Intérêt Régional, Polabfer" (No 2201). We thank Professor Ioav Cabantchik for helpful discussion.

References

Albrecht-Gary A, Crumbliss AL (1998) Coordination chemistry of siderophores: thermodynamics and kinetics of iron chelation and release. Metal Ions Biol Syst 35:239–327

Al-Refaie FN, Wonke B, Hoffbrand AV, Wickens DG, Nortey P, Kontoghiorges GJ (1992) Efficacy and possible adverse effects of the oral iron chelator 1, 2-dimethyl-3-hydroxypyrid-4-one (L1) in thalassemia major. Blood 80:593–599

Bradford MM (1976) A rapid and sensitive method for the quantitation of microgram quantities of protein utilizing the principle of protein-dye binding. Anal Biochem 72:248–254

Brissot P, Loreal O (2002) Role of non-transferrin-bound iron in the pathogenesis of iron overload and toxicity. Adv Exp Med Biol 509:45–53

Brissot P, Wright TL, Ma WL, Weisiger R (1985) Efficient clearance of non-transferrin-bound iron by rat liver. Implications for hepatic iron loading in iron overload states. J Clin Invest 76:1463–1470

Brissot P, Troadec MB, Bardou-Jacquet E, Le Lan C, Jouanolle AM, Deugnier Y, Loreal O (2008) Current approach to hemochromatosis. Blood Rev 22(4):195–210

Buss JL, Torti FM, Torti SV (2003) The role of iron chelation in cancer therapy. Curr Med Chem 10(12):1021–1034

Cappellini MD, Cohen A, Piga A, Bejaoui M, Perrotta S, Agaoglu L, Aydinok Y, Kattamis A, Kilinc Y, Porter J et al (2006) A phase 3 study of deferasirox (ICL670), a once-daily oral iron chelator, in patients with beta-thalassemia. Blood 107(9):3455–3462

Cerec V, Glaise D, Garnier D, Morosan S, Turlin B, Drenou B, Gripon P, Kremsdorf D, Guguen-Guillouzo C, Corlu A (2007) Transdifferentiation of hepatocyte-like cells from the human hepatoma HepaRG cell line through bipotent progenitor. Hepatology 45(4):957–967

Chenoufi N, Huber N, Loréal O, Morel I, Pasdeloup N, Cillard J, Brissot P, Lescoat G (1995) Inhibition of iron toxicity in rat and human hepatocyte cultures by the hydroxypyridin-4-ones CP20 and CP94. J Hepatol 23:166–173

Chenoufi N, Drénou B, Loréal O, Pigeon C, Brissot P, Lescoat G (1998) Antiproliferative effect of deferiprone on the HepG2 cell line. Biochem Pharmacol 56:431–437

Collins AF, Fassos FF, Stobie S, Lewis N, Shaw D, Fry M, Templeton DM, McClelland R, Koren G, Olivieri NF (1994) Iron-balance and dose-response studies of the oral iron chelator 1, 2-dimethyl-3-hydroxypyrid-4-one (L1) in iron-loaded patients with sickle cell disease. Blood 83:2329–2333

De Silva DM, Askwith CC, Kaplan J (1996) Molecular mechanisms of iron uptake in eukaryotes. Physiol Rev 76:31–47

Deugnier Y, Loréal O, Turlin B, Guyader D, Jouanolle H, Moirand R, Jacquelinet C, Brissot P (1992) Liver pathology in genetic hemochromatosis: a review of 135 homozygous cases and their bioclinical correlations. Gastroenterology 102:2050–2059

Deugnier Y, Guyader D, Crantok L, Lopez JM, Turlin B, Yaouang J, Jouanolle H, Campion JP, Launois B, Halliday JW et al (1993) Primary liver cancer in genetic

hemochromatosis: a clinical, pathological and pathogenetic study of 54 cases. Gastroenterology 1104:228–234

Gaboriau F, Chantrel-Groussard K, Rakba N, Loyer P, Pasdeloup N, Hider RC, Brissot P, Lescoat G (2004) Iron mobilization, cytoprotection and inhibition of cell proliferation in normal and transformed rat hepatocyte cultures by the hydroxypyridinone CP411, compared to CP20: a biological and physicochemical study. Biochem Pharmacol 67:1479–1487

Glickstein H, El RB, Shvartsman M, Cabantchik ZI (2005) Intracellular labile iron pools as direct targets of iron chelators: a fluorescence study of chelator action in living cells. Blood 106(9):3242–3250

Glickstein H, El RB, Link G, Breuer W, Konijn AM, Hershko C, Nick H, Cabantchik ZI (2006) Action of chelators in iron-loaded cardiac cells: accessibility to intracellular labile iron and functional consequences. Blood 108(9):3195–3203

Gripon P, Rumin S, Urban S, Le Seyec J, Glaise D, Cannie I, Guyomard C, Lucas J, Trepo C, Guguen-Guillouzo C (2002) Infection of a human hepatoma cell line by hepatitis B virus. Proc Natl Acad Sci USA 99(24):15655–15660

Huang XP, Spino M, Thiessen JJ (2006) Transport kinetics of iron chelators and their chelates in Caco-2 cells. Pharm Res 23(2):280–290

Kontoghiorghes GJ (1986) Iron mobilization from ferritin using alpha-oxohydroxy heteroaromatic chelators. Biochem J 233(1):299–302

Kontoghiorghes GJ, Evans RW (1985) Site specificity of iron removal from transferrin by alpha-ketohydroxypyridine chelators. FEBS Lett 189(1):141–144

Kontoghiorghes GJ, Goddard JG, Bartlett AN, Sheppard L (1990) Pharmacokinetic studies in humans with the oral iron chelator 1, 2-dimethyl-3-hydroxypyrid-4-one. Clin Pharmacol Ther 48(3):255–261

Kushner JP, Porter JP, Olivieri NF (2001) Secondary iron overload. Hematology/the education program of the American Society of Hematology American Society of Hematology, pp 47–61

Lescoat G, Chantrel-Groussard K, Pasdeloup N, Nick H, Brissot P, Gaboriau F (2007) Antiproliferative and apoptotic effects in rat and human hepatoma cell cultures of the orally active iron chelator ICL670 compared to CP20: a possible relationship with polyamine metabolism. Cell Prolif 40(5):755–767

Mamtani M, Kulkarni H (2008) Influence of iron chelators on myocardial iron and cardiac function in transfusion-dependent thalassaemia: a systematic review and meta-analysis. Br J Haematol 141(6):882–890

Muckenthaler MU, Galy B, Hentze MW (2008) Systemic iron homeostasis and the iron-responsive element/iron-regulatory protein (IRE/IRP) regulatory network. Annu Rev Nutr 28:197–213

Olivieri NF, Koren G, Matsui D, Liu PP, Blendis L, Cameron R, McClelland RA, Templeton DM (1992) Reduction of tissue iron stores and normalization of serum ferritin during treatment with the oral iron chelator L1 in thalassemia intermedia. Blood 79(10):2741–2748

R'Zik S, Beguin Y (2001) Serum soluble transferrin receptor concentration is an accurate estimate of the mass of tissue receptors. Exp Hematol 29(6):677–685

Richardson DR (1997) Potential of iron chelators as effective antiproliferative agents. Can J Physiol Pharmacol 75(10–11):1164–1180

Richardson DR, Milnes K (1997) The potential of iron chelators of the pyridoxal isonicotinoyl hydrazone class as effective antiproliferative agents II : the mechanism of action of ligands derived from salicylaldehyde benzoyl hydrazone and 2-hydroxy-1-naphthylaldehyde benzoyl hydrazone. Blood 89:3025–3038

Rodbard D, McClean SW (1977) Automated computer analysis for enzymemultiplied immunological techniques. Clin Chem 23(1):112–115

Rouan MC, Marfil F, Mangoni P, Sechaud R, Humbert H, Maurer G (2001) Determination of a new oral iron chelator, ICL670, and its iron complex in plasma by high-performance liquid chromatography and ultraviolet detection. J Chromatogr B Biomed Sci Appl 755(1–2):203–213

Ruhnke M, Ungefroren H, Zehle G, Bader M, Kremer B, Fandrich F (2003) Long-term culture and differentiation of rat embryonic stem cell-like cells into neuronal, glial, endothelial, and hepatic lineages. Stem cells (Dayton, Ohio) 428(4):428–436

Rund D, Rachmilewitz E (2005) Beta-thalassemia. N Engl J Med 353(11):1135–1146

Sohn YS, Breuer W, Munnich A, Cabantchik ZI (2008) Redistribution of accumulated cell iron: a modality of chelation with therapeutic implications. Blood 111(3):1690–1699

Tenopoulou M, Kurz T, Doulias PT, Galaris D, Brunk UT (2007) Does the calcein-AM method assay the total cellular 'labile iron pool' or only a fraction of it? Biochem J 403(2):261–266

Theil EC (1987) Ferritin: structure, gene regulation, and cellular function in animals, plants, and microorganisms. Annu Rev Biochem 56:289–315

Troadec MB, Glaise D, Lamirault G, Le Cunff M, Guerin E, Le Meur N, Detivaud L, Zindy P, Leroyer P, Guisle I et al (2006) Hepatocyte iron loading capacity is associated with differentiation and repression of motility in the HepaRG cell line. Genomics 87(1):93–103

Turlin B, Deugnier Y (2002) Iron overload disorders. Clin Liver Dis 6:481–496

Valle P, Timeus F, Piglione M, Rosso P, di Montezemolo LC, Crescenzio N, Marranca D, Ramenghi U (1995) Effect of different exposures to desferrioxamine on neuroblastoma cell lines. Pediatr Hematol Oncol 12:439–446

Wright TL, Brissot P, Ma WL, Weisiger RA (1986) Characterisation of non-tranferrin-bound iron clearance by rat liver. J Biol Chem 261:10909–10914